SUPPLEMENTAL MATERIAL

Supplemental Methods

Healthy blood donors

Blood samples from healthy donors were collected in 10 mL BD Vacutainer tubes supplemented with K2 EDTA and cells were isolated within the first hour of acquisition. Healthy donors did not take any medication and had neither any defined cardiovascular risk factors nor a chronic or acute disease at the time of blood draw.

Animals and experimental autoimmune myocarditis

LMP2$^{-/-}$ mice were originally provided by HJ Schild [1], LMP7$^{-/-}$ mice by U Steinhoff [2] and LMP2$^{-/-}$/LMP7$^{-/-}$/MECL1$^{-/-}$ (triple-ip$^{-/-}$) mice from Ken Rock to PM Kloetzel [3]. All immunoproteasome-deficient strains were backcrossed into an A/J background for seven to eight generations and female mice were used for induction of TnI-AM. For inhibitor studies, female wt A/J mice were obtained from Envigo (Huntingdon, United Kingdom). To induce TnI-AM, mice were s.c. immunized with a solution of 150 µg murine cardiac TnI-peptide HARVDKVDEERYDVEAKVTKNITEIADLTQKIYDLRGKFK RPTLRRVRIS (Peptide Specialty Laboratories, Heidelberg, Germany) diluted in Complete Freund's Adjuvant (CFA), which was supplemented with 5 mg/mL of *Mycobacterium tuberculosis H37Ra* (Sigma, St Louis, MO, USA). Injections were repeated after 7 and 14 days. If not indicated otherwise, mice were sacrificed after 28 days. Control mice were immunized with CFA+PBS without TnI-peptide. Mice were anesthetized by intraperitoneal injection of 120 mg/kg ketamine and 16 mg/kg xylazine, and sacrificed by cervical dislocation, unless specified otherwise.

Echocardiography

For echocardiography, mice were anesthetized with 1.5-2 % isoflurane and kept warm on a heated platform. Temperature and ECG were monitored continuously. Cardiac function and

morphology were assessed with a VisualSonics Vevo 3100 High-Frequency Imaging System using a high-resolution (44MHz) transducer. Standard imaging planes, M-mode, and functional calculations were obtained. Pulsed wave and tissue Doppler measurements were acquired from a modified apical two-chamber view on the mitral valve. For parasternal long axis LV Trace, the average systolic or diastolic volume in B-Mode is be based on the rotational volume of the LV trace at systole or diastole around the long axis line of the spline. The parasternal long-axis view of the left ventricle (LV) was used to guide calculations of ventricular dimensions (M-mode), volumes (B mode; LV Vol; d = LV trace end-diastolic; LV Vol; s = LV trace end-systolic; stroke volume using the formula $SV = LV\ Vol;d - LV\ Vol;s$) and left ventricular ejection fraction (B mode using the formula $LVEF = 100x(\frac{LV\ Vol;s - LV\ Vol;d}{LV\ Vol;d})$). Images in short-axis view were acquired at the mid-papillary level of the left ventricle for calculation of fractional area shortening (FAC, % fractional area change, B mode) using the formula $FAC = 100x(\frac{end-diastolic\ area - end-systolic\ area}{end-diastolic\ area})$. M-mode echocardiographic images were recorded at the level of the papillary muscles from the parasternal short-axis view. All measurements were performed by an experienced, blinded technician of the echocardiography core laboratory of the Max-Delbrück-Center for Molecular Medicine.

Histology

Mouse hearts were removed, fixed in 10 % neutral buffered formalin and subsequently embedded in paraffin. Sections of 3-5 µm thickness were cut and stained with hematoxylin and eosin (HE) to determine the inflamed area. In addition, acid fuchsin orange g (Afog) staining was performed to detect collagen deposition. Five sections of each heart were inspected in a double-blinded fashion by two independent investigators under light microscopy to determine respective inflammation and fibrosis scores as described elsewhere [4]. Human endomyocardial biopsies were stored and stained with HE as described elsewhere [5] and stained with antibodies

for LMP2 (1:600, rabbit polyclonal, Abcam) [6], LMP7 (1:500, PW8845, Enzo) [7], IL-17 (5 µg/ml R&D Systems, AF-317-NA). As detection system, we used VisUCyte HRP Polymer Mouse/Rabbit (LMP2, LMP7) resp. goat (IL-17) from R&D, Minneapolis followed by staining with HistoGreen (Linaris, Dossenheim) as substrate. For immunohistological detection of cardiac immune cells a monoclonal CD3 antibody (rabbit, clone 2GV6, Roche, Basel), a monoclonal CD68 antibody (mouse, clone PG-M1, 1:50, DAKO, Hamburg, Germany) were used. A polyclonal rabbit anti-human IgG (1:30.000, A0423, DAKO, Hamburg, Germany) was used to visualize IgG. Immunohistochemical analysis was performed on an automated immunostainer following the manufacturer's protocol (Benchmark; Ventana Medical Systems, Tucson, AZ) and using the ultraView detection system (Ventana) and diaminobenzidine as substrate. Tissue sections were counterstained with hematoxylin.

Cell culture, isolation of immune cells from mouse tissue and human monocytes

Splenocytes were prepared by passing spleen tissue trough a 70 µm cell strainer (BD Bioscience). After a wash step with 1x PBS, RBC lysis was performed 2-3 time in a row by incubating with 0.83% ammonium chloride (NH_4Cl) for 3-5 min at room temperature. Cells were recovered by centrifugation (10 min, 310 g), re-suspended in FACS buffer, and chilled on ice until flow cytometry. Fresh whole blood was 1:2 diluted with pyrogen-free PBS, which was overlayed onto a Ficoll-Paque density solution (d=1.077; GE Healthcare). Peripheral blood mononuclear cells (PBMC) were retrieved by density centrifugation for 30 min at 500 g with reduced acceleration and no break at room temperature. Thereafter, the PBMC containing layer was washed with PBS and platelets were removed by two consecutive centrifugation steps at 100 g for 15 min at 4 °C. $CD14^+$ cells were purified through positive selection with magnetic cell sorting (MACS) using magnetic-labelled $CD14^+$ beads (Miltenyi Biotec). From this time point on, monocytes were always kept on ice and purified $CD14^+$ monocytes were suspended in RPMI medium (GIBCO) plus 2% human AB serum (SIGMA) plus HEPES, sodium-

pyruvate, glutamine and penicillin/streptomycin at a concentration of $1x10^6$/mL. 5x10^5 cells were plated in 24-well format and incubated at 37°C and 100 rpm for 1 hour. Cells were treated with 200 nM ONX 0914 (Selleckchem, San Diego, CA, USA or Cayman Chemicals, MI, USA) or DMSO for 1 hour [8] prior to stimulation with R848 (10 µg/mL, Stemcell Technologies), Pam3CK4 (0.2 µg/mL, Invivogen), LPS (0.5 µg/ml + 2 nM ATP) for another 4 hours.

For heart tissue, after extraction of whole blood the heart was flushed with 15 mL PBS, removed and washed again in PBS. An in terms of weight defined amount of heart tissue was minced in RPMI 1640 medium (Biochrom) containing 10 % (v/v) fetal calf serum (FCS) (Biochrom), 1 % (v/v) penicillin/streptomycin (Pan Biotech), 30 mM HEPES, 0.1 % (w/v) collagenase type 2 (Worthington) and 0.015 % (w/v) DNase I (Sigma-Aldrich). Tissue digestion occurred during incubation at 37 °C for 30 min (shaking at 800 rpm). In order to obtain single-cell status, 10 mM EDTA were added, cells were washed with PBS, and were passed through a 70 µm cell strainer (BD Bioscience). Cells were recovered by centrifugation (10 min, 310 g), re-suspended in FACS buffer, and chilled on ice until flow cytometry.

Proteasome inhibitor and treatment protocols

ONX 0914 is a cell-permeable immunoproteasome-selective inhibitor (Onyx Pharmaceuticals/Amgen South San Francisco, CA or Selleckchem, San Diego, CA, USA). ONX 0914 was formulated in an aqueous solution of 10 % (w/v) Captisol™ (Ligand Pharmaceuticals SanDiego, CA) and 10 mM sodium citrate (pH 6). The solution was s.c. administered to mice three times a week at a dose of 10 mg/kg. Control group animals received matching amounts of Captisol-sodium citrate mix (referred to as vehicle).

Detection of serum concentrations of anti-cardiac TnI-peptide titers

Mice: 96-well cell culture plates were coated with 100 µL per well of cardiac TnI-peptide (5µg/mL) diluted in bicarbonate buffer (pH 9.6) overnight. Serum samples obtained from mice were diluted to 1:800, 1:3.200, 1:12.800, 1:51.200, 1:204.800 and 1:819.200. Horseradish peroxidase conjugated anti-mouse IgG secondary antibody (Sigma) were diluted 1:5.000 and plates were incubated for detection of IgG antibodies directed against TnI. Optical densities were determined at 450 nm. Antibody titers for each individual mouse were calculated as the greatest positive dilution of sera yielding a positive antibody signal as decribed in [9]. Serum from patients: 96-well cell culture plates were coated with 50 µL per well of anti-cardiac TnI antibody (1µg/mL; lab stock) diluted in bicarbonate buffer (pH 9.6) overnight. Afterwards, half of the plate was coated with 50 µL human cTnI (3 µg/mL) in 1× PBS/1% bovine serum albumin (BSA)/0.1% Tween 20, while the other half served as control and was incubated with 1× PBS/1% BSA/0.1% Tween 20. Serum samples were diluted 1:20, 1:40, 1:80, 1:160 and 1:320. Horseradish peroxidase conjugated anti-human IgG secondary antibody (BD) were diluted 1:7.500 and plates were incubated for detection of IgG antibodies directed against cTnI. Optical densities were determined at 450 nm. Antibody titers were calculated as the greatest positive dilution of sera yielding a positive antibody signal as decribed in [9].

Quantitative real-time polymerase chain reaction (qPCR)

Total RNA was isolated from mouse hearts using RNeasy Fibrous Tissue Mini Kit (Qiagen, Hilden, Germany) following the manufacturer's instructions. 1 µg RNA was used for cDNA synthesis (iScript™ gDNA Clear cDNA Synthesis Kit, Bio-Rad, Munich, Germany). mRNA expression was quantified applying iTaq™ universal SYBR® Green supermix (Bio-Rad, Munich, Germany) according to the manufacturer's instructions and using an iCycler iQ2 Detection System (Bio-Rad). 50 ng cDNA was dissolved in a 10 µL reaction volume. A denaturation step at 95 °C was carried out for 5 min, followed by 40 cycles of denaturation at

95 ºC for 10 sec and annealing at 60 ºC for 30 sec. Primer sequences are listed in Table Exp1. Obtained relative mRNA expressions (r) were normalized to the expression of the reference gene L32 as well as to the expression of the respective target gene in CFA-immunized wt mice by the following formula [10]:

$$r = (\frac{E_{target}^{\Delta Ct_{target}(control-sample)}}{E_{ref}^{\Delta Ct_{ref}(control-sample)}}$$

The primer efficiencies (E) were calculated with LinReg 11.1 (J. M. Ruijter, S. van der Velden, A. Ilgun, Heart Failure Research Center (HFRC), Amsterdam, Netherlands). A Ct value of 34.25 was set as a detection limit. If Ct values were above the detection limit, the relative expression was set to zero. For human monocytes, spleen tissue homogenates, and endomyocardial biopsies, total RNA was isolated using Trizol RNA isolation. cDNA synthesis, and quantitative real-time PCR were performed as described in publication [11]. Primers and probes for TaqMan PCR (human: CCL3, CCL4, CXCL2, IL-6, IL-1β, TNF-α; mouse: CD4, CD25, FoxP3, PD1, LMP2, LMP7, IL-17) were purchased from ThermoFisher (TaqManTM Gene Expression Assays). mRNA expression was normalized to the housekeeping gene hypoxanthine-guanine phosphoribosyltransferase (HPRT) according to the ΔCt method and $2^{-\Delta Ct}$ values for each cytokine/chemokine of ONX 0914-treated monocytes from each patient were normalized to the respective DMSO-treated control $2^{-\Delta Ct}$.

Western blot and antibodies

For analysis of the catalytically active proteasomal subunits, spleens were isolated from naive A/J mice, triple-ip$^{-/-}$, LMP2$^{-/-}$, and LMP7$^{-/-}$ mice (n=2 per strain), respectively. For SDS-PAGE tissue lysis was performed using RIPA buffer (20 mM Tris-HCl pH 7.5, 100 mM NaCl, 10 mM EDTA, 1% (v/v) Nonidet P40, 0.1% (w/v) SDS, 10 μM MG132, 5 mM NEM, Complete protease inhibitor cocktail (Roche)). Immunoblot analysis was performed according to standard procedures [34]. Primary antibodies: α4 (K378/1, lab stock), LMP7 (K63, lab stock), LMP2

(Abcam 3328), β5 (Abcam 3330), β1 (lab stock), MECL1 (K65, lab stock), mouse actin (Millipore). The bound primary antibodies were detected using IRDye800CW or IRDye680DT labelled goat anti-mouse/anti-rabbit secondary antibodies in conjunction with an Odyssey CLx infrared imaging system (Li-Cor Biosciences). Alternatively, TnI peptide used for immunization of mice, human TnI or TnT were loaded onto SDS gels (1 µg per lane), and gels were subjected to Western blotting for detection of the respective antigens by serum of patient 3 (100 µg/mL in 5% BSA TBST) and visualization by anti-human IgG IgG HRP DC 555788 as performed in [12].

RNA-Seq analysis, Read processing and Mappings

Endomyocardial biopsies from patient 2 were immediately washed in ice-cold saline (0.9% NaCl), transferred and stored in liquid nitrogen until RNA extraction using an Allprep Kit (Qiagen). Two control samples (Bioserve, USA) were used according to the protected health information (45 C.F.R. 164.514 e2). Biomaterial processing for RNA-seq analysis of heart biopsies was performed as previously described [13]. Sequencing libraries were generated using the TruSeq Stranded Total RNA Sample Preparation Kit with Ribo-Zero Human/Mouse/Rat from Illumina, adhering to the standard protocol of the kit. Sequencing was performed using 2x100bp paired end sequencing on an Illumina NovaSeq instrument. The read libraries were mapped to the human genome, build 38, patch release 5 (GRCh38) using the STAR aligner [14]. For quality control, the programs dupRadar [15], fastqc (https://www.bioinformatics.babraham.ac.uk/projects/fastqc/) and RNA-SeQC [16] were used. Gene counts were obtained using the featureCounts program from the subread package [17]. Genes for which (i) the number of samples with at least three counts in a sample was smaller than 1 or (ii) the variance of number of counts was zero were removed from the analysis. Of 58096 genes, 15400 remained after filtering. Differential expression was analysed with the DESeq2 R package [18]. Data for all 15400 genes are displayed in Table S3. For gene set

enrichment analysis, the R package tmod [19] was used. Alternatively, a gene set entitled autoimmunity was defined as summarized in Table S2.

Flow Cytometry

Either equal numbers of splenocytes or cells purified from 15 mg heart tissue were incubated (20 min at 4 °C) in FACS buffer (1xPBS, 2 % FCS, 2 mM EDTA) containing an anti-mouse Fc receptor blocking reagent (1:50; Miltenyi). Afterwards, fluorochrome-conjugated antibodies against various surface markers were added and incubated for at least 20 min at 4 °C protected from light. The following antibodies were purchased from BD Bioscience: CD8α (FITC; clone 53-6.7), CD62-L (PercP Cy5.5; clone MEL-14), B220 (PE; clone RA3-6B2), CD90.2/Thy-1.2 (PE; clone 53-2.1), TER-119 (PE; clone TER-119), CD11b (PE-CF594; clone M1/70), CD4 (V500; clone RM4-5), CD8α (Pacific Blue™; clone 53.6.7). CD49b (PE; clone DX5), CD44 (PE; clone IM7) and CD3 (APC; clone 2-C11) were purchased from eBioscience. PD-1 (PercP Cy5.5; clone RMP1-30), CD45.2 (Brilliant Violet 711™; clone 104), Ly6G (PerCP/Cy5.5; clone 1A8), Ly6C (Pacific Blue™; clone HK1.4), CD11c (Brilliant Violet 510™; clone N418), F4/80 (APC; clone BM8), CD3 (PerCP/Cy5.5; clone 145-2C11), B220 (FITC; clone RA3-6B2), CD19 (APC; clone 6D5) were purchased from BioLegend. After several wash steps with FACS buffer (centrifugation: 3 min at 300 g), cells were re-suspended in 150 µL of the fixable viability dye eFluor 780 (eBioscience), diluted 1:1.000 in PBS and incubated for 30 min on ice protected from light. After serial wash steps with PBS followed by fixation in FACSFix (1x PBS, 2 % Roth^{TM}Histofix), cells were acquired on either a FACS Symphony flow cytometer (BD Bioscience) or a FACS Canto II flow cytometer (BD Bioscience). Data were analyzed using FlowJo v10.0 software (Tree Star). In order to quantify total cell numbers in heart tissue, 123count eBeads (eBioscience) were used according to manufacturer's protocol. Reported numbers were normalized for the weight of total hearts, yielding the number of respective cell fraction per mg tissue. Monocytes were identified by positive gating on CD45, CD11b and

further exclusion of Ly6G, CD11c and F4/80-positive cells in addition to lineage negative staining (B220, CD90.2, CD49b and Ter-119) as recently described by the Nahrendorf group [20]. Expression of Ly6C was used to further discriminate between patrolling and inflammatory monocytes.

Supplemental Tables

Supplemental Table 1. Effect of ONX 0914 on cardiac function in control mice.

	before treatment		after treatment		
	vehicle	**ONX 0914**	**vehicle**	**ONX 0914**	**p value**
Heart rate [bpm]	365.0 ± 17.8	362.3 ± 8.9	397.2 ± 10.9	353.3 ± 11.8	0.265
Trace LVEF [%]	57.0 ± 2.1	49.5 ± 2.9	52.2 ± 2.7	53.6 ± 1.9	0.873
Stroke volume [µL]	16.7 ± 0.9	16.0 ± 1.1	17.0 ± 1.1	19. 1± 0.8	0.102
Cardiac output [ml/min]	6.1 ± 0.4	5.8 ± 0.5	6.8 ± 0.5	6.8 ± 0.4	0.093
LVID-d [mm]	3.2 ± 0.1	3.3 ± 0.1	3.4 ± 0.0	3.5 ± 0.0	0.078
LVID-s [mm]	2.2 ± 0.1	2.5 ± 0.1	2.4 ± 0.1	2.6 ± 0.1	0.050
MV s´ [mm/s] #	21.9 ± 0.8	18.2 ± 1.0	20.2 ± 1.1	20.4 ± 1.7	0.823
MV E [mm/s] #	667.8 ± 19.8	624.4 ± 37.7	631.6 ± 16.7	615.2 ± 18.1	0.313
MV e´ [mm/s] #	21.8 ± 1.6	19.9 ± 1.7	23.8 ± 2.6	25.9 ± 2.2	0.737
MV E/e´#	31.9 ± 2.1	32.8 ± 2.1	29.9 ± 3.8	25.5 ± 2.0	0.391
MV ejection time [ms] #	51.1 ± 1.1	49.5 ± 0.7	49.1 ± 0.9	52.1 ± 1.1	0.813
MV_{decel} [ms] #	25.0 ± 1.6	25.6 ± 1.3	25.6 ± 0.9	27.1 ± 1.2	0.297
IVRT [ms]#	19.0 ± 0.7	17.9 ± 0.5	19.7 ± 0.4	20.6 ± 0.6	0.522

Female A/J mice were divided in two groups: vehicle and ONX 0914 (n=12 vehicle; n=12 ONX 0914). Prior to vehicle or ONX 0914 treatment, cardiac function was determined by echocardiography using a Vevo3100 machine. Afterwards, mice were treated with 10 mg/kg ONX 0914 or vehicle s.c., and a second echocardiography was performed after 48 hours. Data are summarized as mean ± SEM. Repeated measurements two-way ANOVA was performed, and, if two-way ANOVA revealed a significant effect, depicted p values reflect results obtained from a Sidak's multiple comparison test comparing vehicle vs. ONX 0914-treated mice. LVEF: left ventricular ejection fraction; LVID-d/s: left ventricle internal diameter at diastole/systole; bpm: beats per minute; MV_{decel}: deceleration time; IVRT: isovolumic relaxation time; IVRT, MV_{ET}; MV_{decel}, Mitral valve E velocity were determined by pulse-wave Doppler at mitral valve. Peak mitral valve e´ and s´ velocity were determined by tissue Doppler imaging. # Parameters to assess diastolic function of the left ventricle.

Supplemental Table 2. Definition of the "autoimmunity" gene set for gene enrichment analysis of RNASeq data. Gene identification from HUGO (human gene nomenclature committee).

	title	**gene identification**
immunoproteasome	LMP2	9546
	LMP7	9545
	MECL1	9538
T-cell response	CD3 (epsilon)	1674
	CD4	1678
	ROR-γt[*1]	10260
	IL17	5981
	IL2	6001
	IFNγ	5438
B-cell response	IgG heavy chain[*2]	5525
	IgG light chain κ[*3]	5716
	IgG light chain λ[*4]	5855
	CD19	1633
	PTPRC[*5]	9666
monocytes	CD14	1628
	TLR2	11848
	TLR8	15632
pro-inflammatory cytokines	IL6	6018
	IL1β	5992
	TNFα	11892
chemokines	CCL2	10618
	CCL3	10627
	CCL4	10630
	CCL5	10632
	CXCL2	4603
chemokine receptors	CCR1	1602
	CCR2	1603
	CCR5	1606

*1 RAR related orphan receptor C- γt; *2 immunoglobulin heavy constant gamma 1 (G1m marker); *3 immunoglobulin kappa constant; *4 immunoglobulin light chain constant 1; *5 PTPRC (protein tyrosine phosphatase receptor type C), B220

Supplemental Table 3. RNA seq analysis of endomyocardial biopsies from patient 2. Biomaterial processing for RNA-seq analysis of heart biopsies from patient 2 and two control samples (Bioserve, USA) was performed as previously described [13]. Of 58096 genes, 15400 remained after filtering. The table displays the differential expression for all 15400 genes analyzed with the DESeq2 R package [18].

Supplemental Figures and Figure Legends

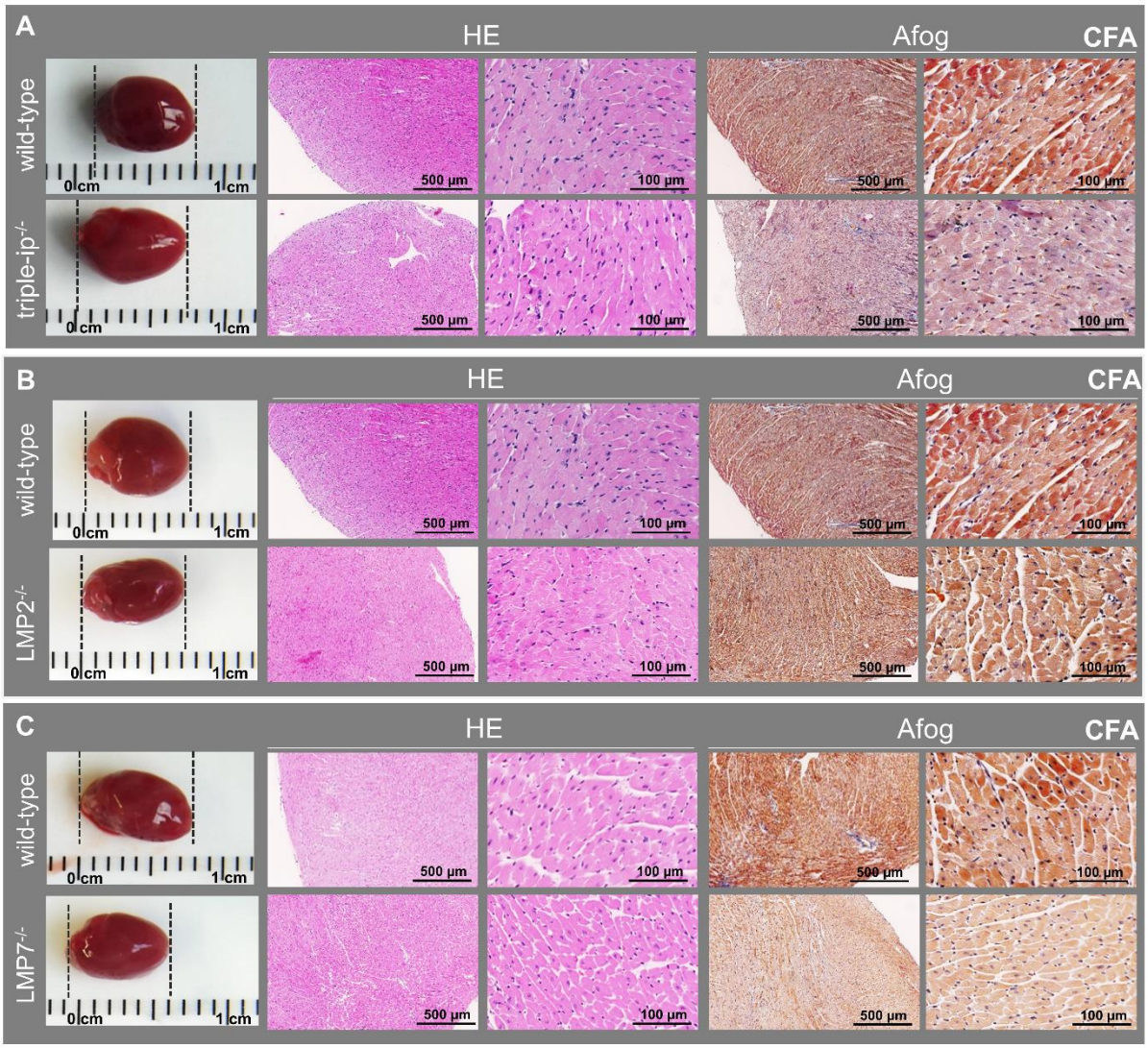

Supplemental Figure 1

Non-peptide, CFA-immunized triple-ip$^{-/-}$, LMP2$^{-/-}$ and LMP7$^{-/-}$ demonstrate reveal no signs of cardiac inflammation. (A) Triple-ip$^{-/-}$ (n=4), (B) LMP2$^{-/-}$ (n=5) and (C) LMP7$^{-/-}$ (n=5) as well as their respective wild-type controls were immunized with CFA (no TnI peptide) on day 0, 7 and 14. Mice were sacrificed for analysis after 28 days. Photographs of mouse hearts representative for all four groups are depicted. Next, paraffin-embedded heart tissue sections were prepared and stained using HE or Afog. Representative images are shown for each group.

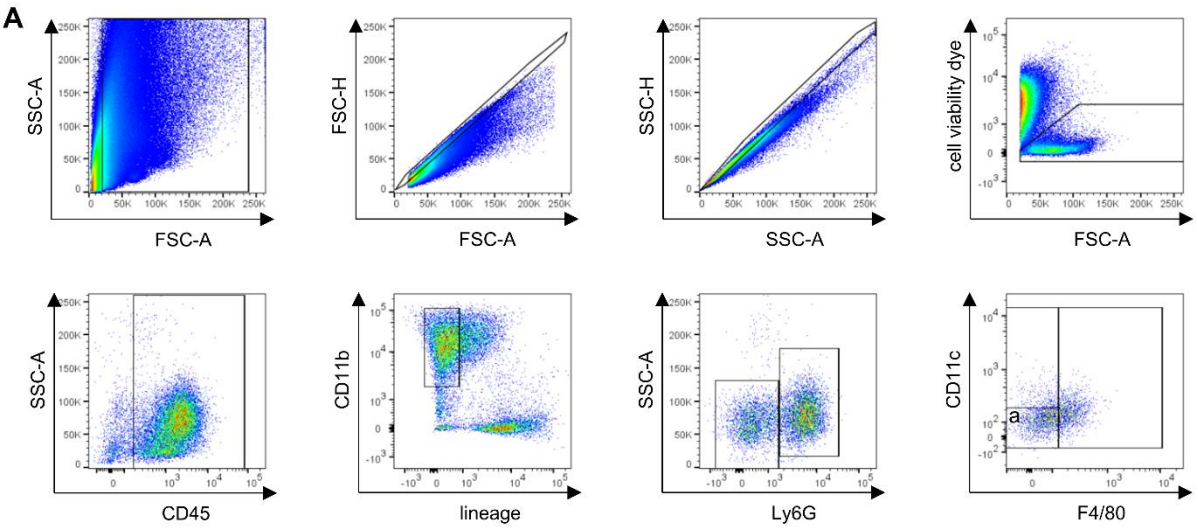

monocytes: single cells, cell viability dye^{low}, CD45^{+}, CD11b^{high}, lineage^{-} (B220^{-}, CD90.2^{-}, CD49b^{-}, Ter-119^{-}), Ly6G^{-}, CD11c^{-}, F4/80^{-}
inflammatory monocytes: single cells, cell viability dye^{low}, CD45^{+}, CD11b^{high}, lineage^{-} (B220^{-}, CD90.2^{-}, CD49b^{-}, Ter-119^{-}), Ly6G^{-}, CD11c^{-}, F4/80^{-} , Ly6C^{high}
patrolling monocytes: single cells, cell viability dye^{low}, CD45^{+}, CD11b^{high}, lineage^{-} (B220^{-}, CD90.2^{-}, CD49b^{-}, Ter-119^{-}), Ly6G^{-}, CD11c^{-}, F4/80^{-} , Ly6C^{high}
macrophages: single cells, cell viability dye^{low}, CD45^{+}, CD11b^{high}, lineage^{-} (B220^{-}, CD90.2^{-}, CD49b^{-}, Ter-119^{-}), Ly6G^{-}, CD11c$^{+/-}$, F4/80^{+}
dendritic cells: single cells, cell viability dye^{low}, CD45^{+}, CD11b^{high}, lineage^{-} (B220^{-}, CD90.2^{-}, CD49b^{-}, Ter-119^{-}), Ly6G^{-}, CD11c^{+}, F4/80^{-}
neutrophils: single cells, cell viability dye^{low}, CD45^{+}, CD11b^{high}, lineage^{-} (B220^{-}, CD90.2^{-}, CD49b^{-}, Ter-119^{-}), Ly6G^{+}

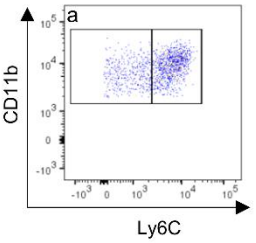

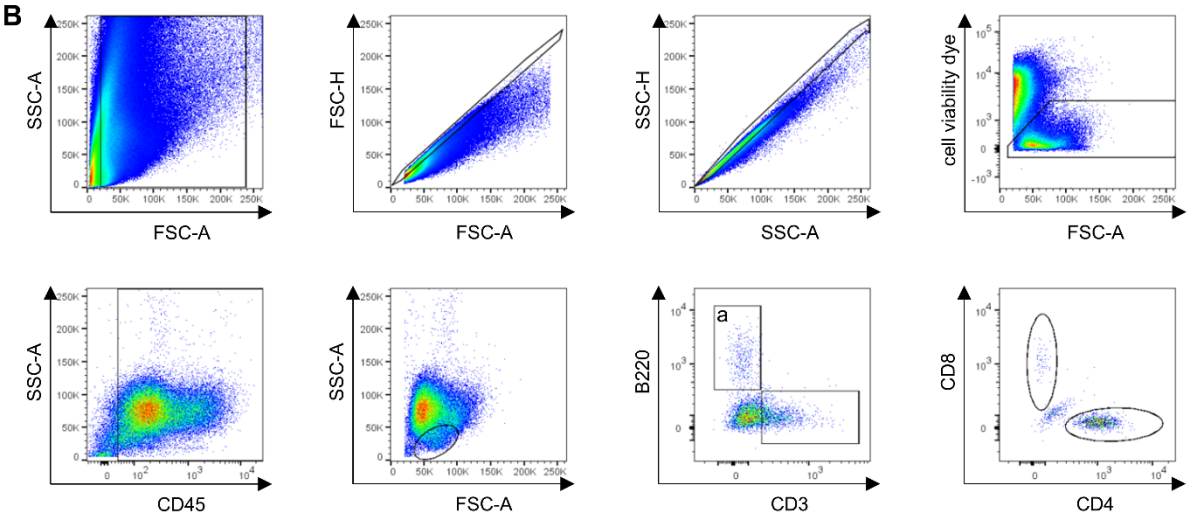

T cells: single cells, cell viability dye^{low}, CD45^{+}, FSC-A^{low}, SSC-A^{low}, B220^{-}, CD3^{+} and CD8^{+} or CD4^{+}
CD4^{+} T cells: single cells, cell viability dye^{low}, CD45^{+}, FSC-A^{low}, SSC-A^{low}, B220^{-}, CD3^{+}, CD8^{-}, CD4^{+}
CD8^{+} T cells: single cells, cell viability dye^{low}, CD45^{+}, FSC-A^{low}, SSC-A^{low}, B220^{-}, CD3^{+}, CD8^{+}, CD4^{-}
B cells: single cells, cell viability dye^{low}, CD45^{+}, FSC-A^{low}, SSC-A^{low}, CD3^{-} ,B220^{+}, CD19^{+}

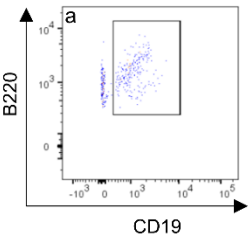

Supplemental Figure 2

Gating strategy for immune cells during TnI-AM. Cells were first gated on size, granularity and singularity followed by viability dye exclusion to identify live cells for further analysis. (A) Myeloid cell characterization strategy: Live cells were gated on the expression of CD45 and further of CD11b to identify myeloid cells. NEUTROPHILS were identified as single cells, cell viability dye^{low}, CD45^{+}, CD11b^{high}, lineage^{-} (B220^{-}, CD90.2^{-}, CD49b^{-}, Ter-119^{-}), Ly6G^{+}. Non-neutrophil (Ly6G^{-}) myeloid cells were discriminated additionally by assessing the expression both of F4/80 and CD11c as MACROPHAGES (single cells, cell viability dye^{low}, CD45^{+}, CD11b^{high}, lineage^{-} (B220^{-}, CD90.2^{-}, CD49b^{-}, Ter-119^{-}), Ly6G^{-}, CD11c$^{+/-}$, F4/80^{+}), DENDRITIC CELLS (single cells, cell viability dye^{low}, CD45^{+}, CD11b^{high}, lineage^{-} (B220^{-}, CD90.2^{-}, CD49b^{-}, Ter-119^{-}), Ly6G^{-}, CD11c^{+}, F4/80^{-}) and monocytes. MONOCYTES were identified as Fixable Viability Dye^{low} , CD45.2^{+}, CD11b^{high}, lineage (B220, CD90.2, CD49, Ter-119)$^{–}$, Ly6G$^{–}$, SSC^{low}, F4/80$^{–}$/CD11c$^{–}$. Monocytes were further differentiated according to expression of Ly6C as INFLAMMATORY MONOCYTES (single cells, cell viability dye^{low}, CD45^{+}, CD11b^{high}, lineage^{-} (B220^{-}, CD90.2^{-}, CD49b^{-}, Ter-119^{-}), Ly6G^{-}, CD11c^{-}, F4/80^{-} , Ly6C^{high}) and PATROLLING MONOCYTES (single cells, cell viability dye^{low}, CD45^{+}, CD11b^{high}, lineage^{-} (B220^{-} , CD90.2^{-}, CD49b^{-}, Ter-119^{-}), Ly6G^{-}, CD11c^{-}, F4/80^{-} , Ly6C^{high}). (B) Lymphoid cell characterization strategy: Live cells were gated on the expression of CD45 and further by size and singularity to exclude auto-fluorescent neutrophils. Cells were then gated on B220 and CD3 expression to identify lymphocytes. CD3 expressing B220 negative T cells were further discriminated by additional assessment of CD8 and CD4. T CELLS: single cells, cell viability dye^{low}, CD45^{+}, FSC-A^{low}, SSC-A^{low}, B220^{-}, CD3^{+} and CD8^{+} or CD4^{+}. CD4^{+} T CELLS: single cells, cell viability dye^{low}, CD45^{+}, FSC-A^{low}, SSC-A^{low}, B220^{-}, CD3^{+}, CD8^{-}, CD4^{+}. CD8^{+} T CELLS: single cells, cell viability dye^{low}, CD45^{+}, FSC-A^{low}, SSC-A^{low}, B220^{-}, CD3^{+}, CD8^{+}, CD4^{-}. B CELLS:: single cells, cell viability dye^{low}, CD45^{+}, FSC-A^{low}, SSC-A^{low}, CD3^{-} ,B220^{+}, CD19^{+}.

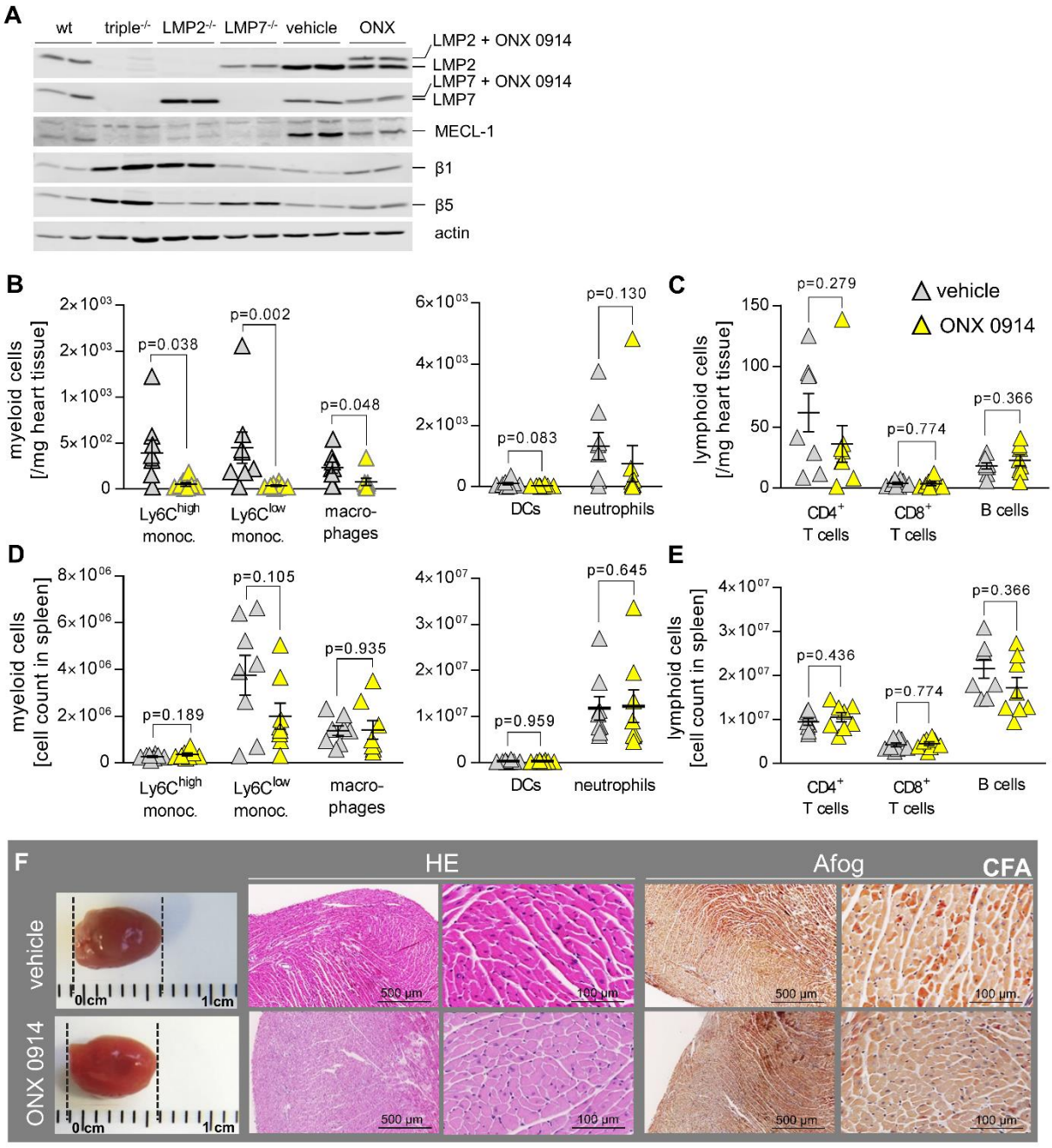

Supplemental Figure 3

Immune cell abundance in heart and spleen after ONX 0914 treatment during TnI-AM.

(A) Splenic homogenates obtained from naive wt, triple-ip$^{-/-}$, LMP2$^{-/-}$, LMP7$^{-/-}$ mice were used for Western blotting for the indicated proteasome subunits. The results of the Western blot analysis demonstrate an increase of the standard proteasome as mirrored by higher expression of β1 and β5 expression upon deletion of immunoproteasome subunits in immunoproteasome-deficient mice. Such biological compensatory aspects might camouflage the pathological

function of immunoproteasome peptidase activity in autoimmunity [21]. In addition, wt A/J mice were divided into two groups that received either vehicle or ONX 0914 three times per week starting a day prior to the first TnI immunization. On day 7 and 14, mice received a second and third immunization, respectively. Mice were sacrificed for analysis 25 and 26 days after the first immunization (equal distribution of both treatment groups). Splenic homogenates from two mice per group are shown representatively. An upward shift indicates inhibition of the respective subunit by ONX 0914. The immunoproteasome inhibitor affected the formation of the immunoproteasome also, and treatment had compensatory effects resulting in higher expression of β1 and β5 standard proteasome subunits **(Fig 5A)**. (B/C) To analyze infiltration with immune cells in ONX 0914-treated mice, single cell solutions from heart tissue were generated and analyzed by flow cytometry. (D/E) Since immunoproteasome function controls the mobilization of myeloid cells from the bone marrow and their sequestration in the spleen [22], but also influences T cell survival [23, 24], we investigated whether ONX 0914 influenced lymphocyte and myeloid cell abundance in the spleen during TnI-AM. A detailed gating strategy is depicted in **Fig S2**. Myeloid cells were identified as single cells, cell viability dye^{low}, $CD45^{+}$, $CD11b^{high}$ and $lineage^{-}$ (lineage markers used were: B220, CD90.2, CD49b and Ter-119). Herein, monocytes were defined as $Ly6G^{-}$, $CD11c^{-}$ and $F4/80^{-}$ as described elsewhere [20]. CD11c and F4/80 was gated strictly negative using internal negative controls (single cells, cell viability dye^{low}, $CD45^{+}$, $CD11b^{-}$, $lineage^{+}$). Inflammatory monocytes were defined by additional expression of Ly6C. Myeloid cells were defined prior to allocation to either neutrophils and dendritic cells. Lymphoid cells were gated regarding the expression of B220, CD19, CD3, CD4 and CD8. n=10 for vehicle and n=10 ONX 0914. Heart tissue: For all myeloid cells, data are median ± interquartile range. A Mann-Whitney-test was performed. All other data are mean ± SEM and a t-test was performed. P values are indicated in each graph. (F) A/J mice were divided into two groups that received either vehicle or ONX 0914 three times per week starting a day prior to the immunization with CFA (no TnI peptide). On day 7 and 14,

mice received a second and third CFA injection, respectively. Mice were sacrificed for analysis 25 and 26 days after the first immunization (equal distribution of both treatment groups). Photographs of mouse hearts representative for both groups are depicted. Paraffin-embedded heart tissue sections were prepared and stained using HE or Afog. Representative images are shown for each group.

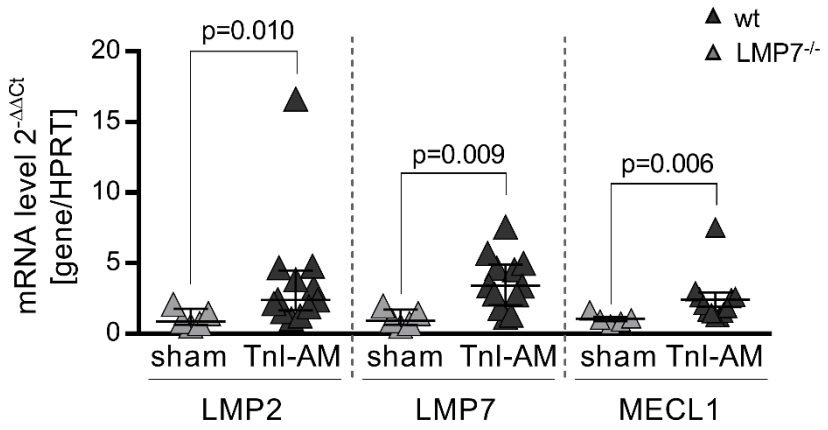

Supplemental Figure 4

mRNA expression levels of the indicated target genes (LMP2, LMP7 and MECL1 are proteases of the immunoproteasome) determined in cardiac tissue in wt mice during TnI-AM (n=12). Data normalized to respective non-peptide, CFA-treated controls (n=5) using the $2^{-\Delta\Delta Ct}$ method. Data are plotted as mean ± SEM and a *t*-test was performed.

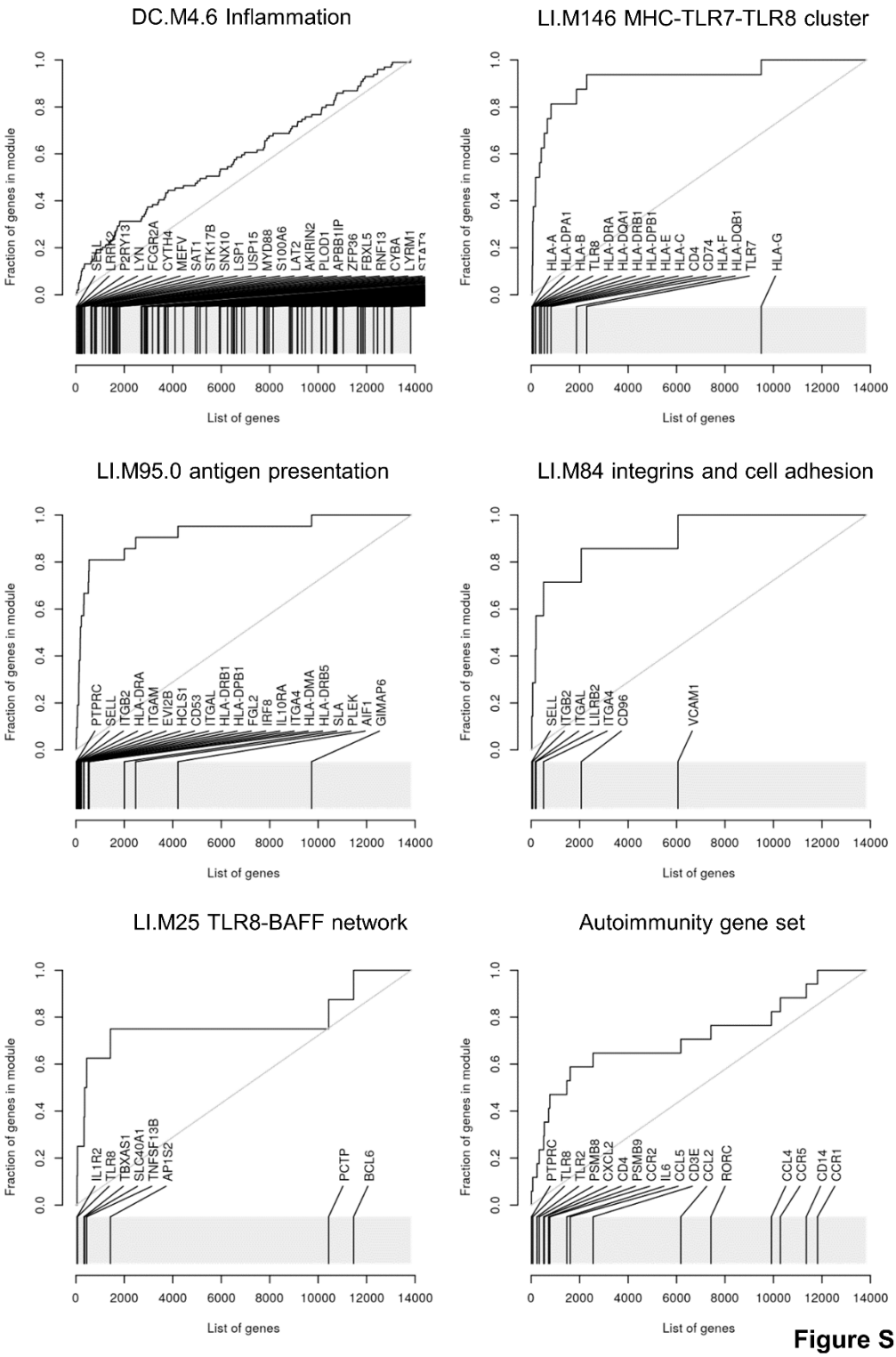

Figure Supplement 5

Supplemental Figure 5

Receiver-operator characteristic (ROC) curve of significantly enriched gene sets from the tmod package [19] and the autoimmunity gene set. X-axis and the grey bar under the curve represents the list of genes ordered by the p-value in the comparison of cardiac transcriptome between

patient 2 and controls. Vertical dashes indicate genes, which were included in the gene sets and their position in the list of transcripts. Vertical axis shows the fraction of the genes in the gene set. Area under the ROC curve (area under curve, AUC) represents the enrichment strength (effect size for the gene set enrichment). BAFF: B cell activating factor

Supplemental References

1. Vankaer L, Ashtonrickardt PG, Eichelberger M, Gaczynska M, Nagashima K, Rock KL, Goldberg AL, Doherty PC and Tonegawa S. Altered Peptidase and Viral-Specific T-Cell Response in Lmp2 Mutant Mice. *Immunity*. 1994;1:533-541.
2. Fehling HJ, Swat W, Laplace C, Kuhn R, Rajewsky K, Muller U and Vonboehmer H. Mhc Class-I Expression in Mice Lacking the Proteasome Subunit Lmp-7. *Science*. 1994;265:1234-1237.
3. Kincaid EZ, Che JW, York I, Escobar H, Reyes-Vargas E, Delgado JC, Welsh RM, Karow ML, Murphy AJ, Valenzuela DM, et al. Mice completely lacking immunoproteasomes show major changes in antigen presentation. *Nat Immunol*. 2012;13:129-135.
4. Bangert A, Andrassy M, Muller AM, Bockstahler M, Fischer A, Volz CH, Leib C, Goser S, Korkmaz-Icoz S, Zittrich S, Jungmann A, Lasitschka F, et al. Critical role of RAGE and HMGB1 in inflammatory heart disease. *Proc. Natl. Acad. Sci. USA*. 2016;113:E155-164.
5. Rahnefeld A, Klingel K, Schuermann A, Diny NL, Althof N, Lindner A, Bleienheuft P, Savvatis K, Respondek D, Opitz E, et al. Ubiquitin-Like Protein ISG15 (Interferon-Stimulated Gene of 15 kDa) in Host Defense Against Heart Failure in a Mouse Model of Virus-Induced Cardiomyopathy. *Circulation*. 2014;130:1589-1600.
6. Keller IE, Vosyka O, Takenaka S, Kloß A, Dahlmann B, Willems LI, Verdoes M, Overkleeft HS, Marcos E, Adnot S, et al. Regulation of Immunoproteasome Function in the Lung. *Sc Rep*. 2015;5:10230.
7. Orre M, Kamphuis W, Dooves S, Kooijman L, Chan ET, Kirk CJ, Dimayuga S, V, Koot S, Mamber C, Jansen AH, et al. Reactive glia show increased immunoproteasome activity in Alzheimer's disease. *Brain*. 2013;136:1415-1431.
8. Muchamuel T, Basler M, Aujay MA, Suzuki E, Kalim KW, Lauer C, Sylvain C, Ring ER, Shields J, Jiang J, et al. A selective inhibitor of the immunoproteasome subunit LMP7 blocks cytokine production and attenuates progression of experimental arthritis. *Nat Med*. 2009;15:781-787.
9. Kaya Z, Goser S, Buss SJ, Leuschner F, Ottl R, Li J, Volkers M, Zittrich S, Pfitzer G, Rose NR et al. Identification of Cardiac Troponin I Sequence Motifs Leading to Heart Failure by Induction of Myocardial Inflammation and Fibrosis. *Circulation*. 2008;118:2063-2072.
10. Pfaffl MW. A new mathematical model for relative quantification in real-time RT-PCR. *Nucleic Acids Res*. 2001;29:e45.
11. Paeschke A, Possehl A, Klingel K, Voss M, Voss K, Kespohl M, Sauter M, Overkleeft HS, Althof N, Garlanda C and Voigt A. The immunoproteasome controls the availability of the cardioprotective pattern recognition molecule Pentraxin3. *Eur J Immunol*. 2016;46:619-633.
12. Voigt A, Bartel K, Egerer K, Trimpert C, Feist E, Gericke C, Kandolf R, Klingel K, Kuckelkorn U, Stangl K et al. Humoral anti-proteasomal autoimmunity in dilated cardiomyopathy. *Bas Res Cardiol*. 2010;105:9-18.
13. Meder B, Haas J, Sedaghat-Hamedani F, Kayvanpour E, Frese K, Lai A, Nietsch R, Scheiner C, Mester S, Bordalo DM et al. Epigenome-Wide Association Study Identifies Cardiac Gene Patterning and a Novel Class of Biomarkers for Heart Failure. *Circulation*. 2017;136:1528-1544.
14. Dobin A, Davis CA, Schlesinger F, Drenkow J, Zaleski C, Jha S, Batut P, Chaisson M and Gingeras TR. STAR: ultrafast universal RNA-seq aligner. *Bioinformatics*. 2013;29:15-21.
15. Sayols S, Scherzinger D and Klein H. dupRadar: a Bioconductor package for the assessment of PCR artifacts in RNA-Seq data. *BMC Bioinformatics*. 2016;17:428.
16. DeLuca DS, Levin JZ, Sivachenko A, Fennell T, Nazaire MD, Williams C, Reich M, Winckler W and Getz G. RNA-SeQC: RNA-seq metrics for quality control and process optimization. *Bioinformatics*. 2012;28:1530-1532.

17. Liao Y, Smyth GK and Shi W. The Subread aligner: fast, accurate and scalable read mapping by seed-and-vote. *Nucleic Acids Res*. 2013;41:e108.
18. Love MI, Huber W and Anders S. Moderated estimation of fold change and dispersion for RNA-seq data with DESeq2. *Genome biology*. 2014;15:550.
19. Zyla J, Marczyk M, Domaszewska T, Kaufmann SHE, Polanska J and Weiner J. Gene set enrichment for reproducible science: comparison of CERNO and eight other algorithms. *Bioinformatics*. 2019; 35:5146-5154.
20. Hulsmans M, Sager HB, Roh JD, Valero-Muñoz M, Houstis NE, Iwamoto Y, Sun Y, Wilson RM, Wojtkiewicz G, Tricot B, et al. Cardiac macrophages promote diastolic dysfunction. *J Exp Med*. 2018;215:423-440.
21. Basler M, Mundt S, Muchamuel T, Moll C, Jiang J, Groettrup M and Kirk CJ. Inhibition of the immunoproteasome ameliorates experimental autoimmune encephalomyelitis. *EMBO Mol Med*. 2014;6:226-238.
22. Althof N, Goetzke CC, Kespohl M, Voss K, Heuser A, Pinkert S, Kaya Z, Klingel K and Beling A. The immunoproteasome-specific inhibitor ONX 0914 reverses susceptibility to acute viral myocarditis. *EMBO Mol Med*. 2018;10:200-218.
23. Hensley SE, Zanker D, Dolan BP, David A, Hickman HD, Embry AC, Skon CN, Grebe KM, Griffin TA, Chen WS et al. Unexpected Role for the Immunoproteasome Subunit LMP2 in Antiviral Humoral and Innate Immune Responses. *J Immunol*. 2010;184:4115-4122.
24. Moebius J, van den Broek M, Groettrup M and Basler M. Immunoproteasomes are essential for survival and expansion of T cells in virus-infected mice. *Eur J Immunol*. 2010;40:3439-3449.